

J. D. Clayden¹, Z. Nagy², D. C. Alexander³, and C. A. Clark¹¹Institute of Child Health, University College London, London, England, United Kingdom, ²Wellcome Trust Centre for Neuroimaging, University College London, London, England, United Kingdom, ³Department of Computer Science, University College London, London, England, United Kingdom**Introduction**

This work describes, for the first time, a process for optimising both the standard Stejskal–Tanner (ST) diffusion MR sequence and the dual spin-echo (DSE) sequence, for the specific purpose of directly estimating axon radius or other microstructural properties of white matter. There has been considerable recent interest in the use of diffusion MR for this purpose (e.g. [1,2]). A computational framework has recently been developed which allows diffusion MR sequences to be optimised for estimating the parameters of microstructure-level models [2], although the framework has so far been applied only to the standard Stejskal–Tanner (ST) pulsed-gradient spin-echo diffusion sequence, and only for relatively large gradient strengths and high SNR regimes. However, many clinical scanners cannot achieve such gradient strengths or SNR levels; and the more recently developed DSE sequence is often preferred over the ST sequence in applications because it suffers less from eddy current induced distortions [3]. Hence, in this study we: (1) develop a signal model and optimisation for the DSE sequence; (2) investigate the ability of optimised sequences to recover axon radius information at a modest SNR; and (3) compare the properties of the two sequences with respect to the estimation of axon radius.

Methods

Our model for the signal produced by an ST diffusion sequence is identical to that in [2]. The normalised signal is assumed to arise from a linear combination of restricted intracellular and hindered extracellular components. The hindered component is assumed to be a 3D Gaussian, while the restricted component follows van Gelderen’s model for the MR signal from particles diffusing in parallel straight cylinders, which includes radius as a parameter [4]. For this work, we have extended the van Gelderen equations to model the signal in the DSE sequence. We make no prior assumption about the orientation of the axons represented by these cylinders.

The DSE sequence is more complex than the ST sequence, and has more free parameters. Fig. 1 shows the parameters relevant to our optimisation, which are the lengths of the first three gradient pulses, δ_1 , δ_2 and δ_3 ; and the onset times, t_1 , t_2 and t_3 . The length of the fourth pulse is fixed due to the balance requirement, $\delta_4 = \delta_1 + \delta_2 - \delta_3$. The time τ is the length of time available for the DSE sequence, which is equivalent to the echo time, TE, less the time required for any preparation pulses and for readout. The TE is part of the optimisation, but it is fixed across the set of pulse arrangements that we optimise over. Bounds on each of the parameters were established, allowing us to randomly generate valid DSE sequences for the optimisation. Using the “active imaging” approach described in [2], based on the Cramér–Rao Lower Bound (CRLB), we optimise for a set of four pulse arrangements along 90 noncollinear diffusion directions. We allow a maximum gradient strength of 32 mT m⁻¹, which is easily achievable on most systems, and we assume a baseline SNR of 10 at a TE of 90 ms. We use Markov chain Monte Carlo to sample a posterior distribution over axon radius from a set of simulated measurements, generated for the optimised sequences by the model, with added Rician noise.

The DSE sequence has improved eddy current characteristics compared to the ST sequence, but eddy current effects with a particular time constant can be nullified completely under specific circumstances [5]. We optimised the DSE sequence both with and without this additional constraint to investigate its effect on the CRLBs. The constraint amounts to the fixing of δ_1 relative to the other parameters, and therefore reduces the number of free parameters in each pulse arrangement by one. As in [5], we chose the time constant of the eddy currents to be $0.7/T$, where T is the sum of the four gradient pulse lengths. The ST sequence and two DSE sequences were compared by calculating the normalised CRLB over 500 noncollinear fibre directions, which indicates the level of error expected in estimating the model parameters. Smaller values are therefore preferable.

Results

Fig. 2 shows histograms of axon radii sampled from the simulated data, using the ST and unconstrained DSE sequences. In total 1000 samples were created in each case, spread evenly among 10 fibre directions. The canonical radii used to generate the data were 5 μ m and 10 μ m. Although there is some overlap between the histogram pairs, clear peaks can be seen around the true radius values. Sample variances were very similar across the two sequences at the 5 μ m radius, but higher in the DSE case at 10 μ m. Fig. 3 shows the means and coefficients of variation (CVs) of the normalised CRLBs for each sequence. Means for a particular radius are similar across the three cases, but CVs diverge at smaller radii. Constraining the DSE sequence to null eddy currents seems to have little effect on the calculated CRLBs.

Discussion

In this work we have developed and compared ST and DSE pulse sequences optimised for estimating axon radius, and compared their theoretical suitabilities for the task. We showed that meaningful information about axon radius can, in principle, be recovered at modest SNR and with limited gradient strength. In addition, while we identified no evidence that the DSE sequence clearly provides better estimates of axon radii, the lower variance over the sphere of the CRLBs in this case suggest that the DSE case may be more robust with respect to varying fibre direction when axon radii are small. However, the capacity to null eddy currents using the DSE sequence, with little effect on the CRLBs, is a major practical benefit. The ability to optimise for estimating axon radius while minimising eddy current induced distortions is a significant step forwards.

References: [1] Assaf, Y. et al., *Magn Reson Med* 59:1347 (2008); [2] Alexander, D.C., *Magn Reson Med* 60:439 (2008); [3] Reese, T.G. et al., *Magn Reson Med* 49:177 (2003); [4] Van Gelderen, P. et al., *J Magn Reson Ser B* 103:255 (1994); [5] Heid, O., *Proc ISMRM*, p. 799 (2000).

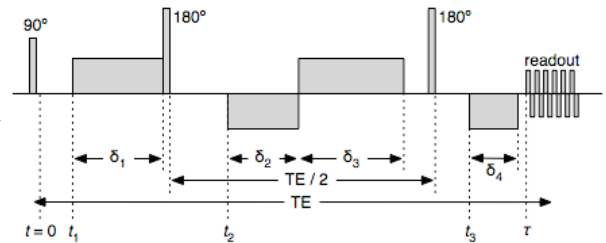


Fig. 1: The dual spin-echo pulse sequence, showing the free parameters of our optimisation.

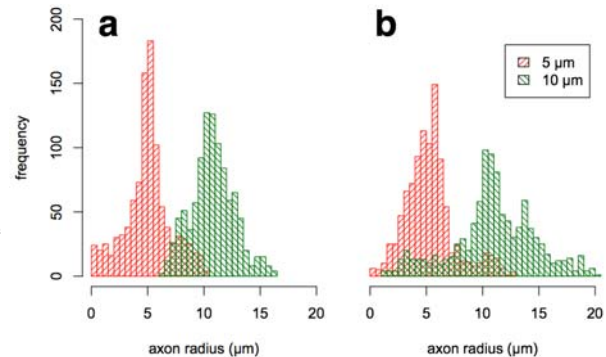


Fig. 2: Histogram of estimated axon radii for the optimised ST (a) and DSE (b) sequences, using canonical radii of 5 μ m and 10 μ m.

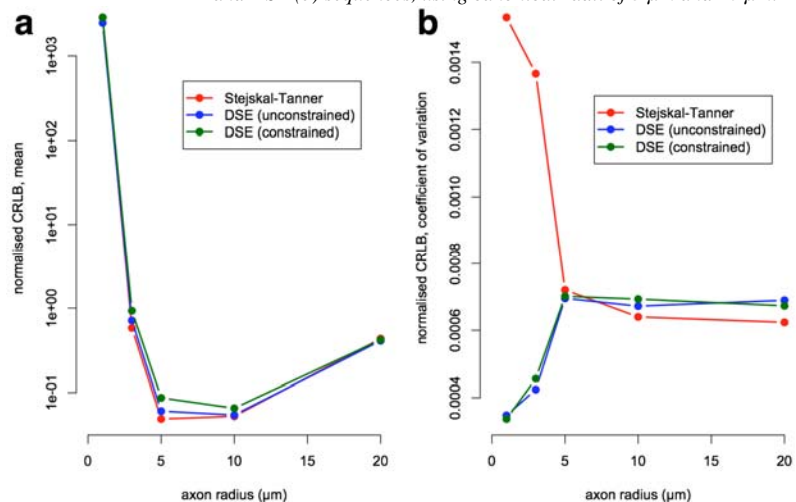


Fig. 3: Means (a) and coefficients of variation (b) for normalised CRLBs obtained for ST and DSE sequences, calculated over 500 fibre directions distributed on a sphere. The constrained DSE sequence includes eddy current nulling.